J_ID: Z7V Customer A_ID: 4295 Cadmus Art: CCI2107 Date: 3-MARCH-05 Stage: II

Catheterization and Cardiovascular Interventions 64:451–459 (2005)

Angiographic Views Used for Percutaneous Coronary Interventions: A Three-Dimensional Analysis of Physician-Determined vs. Computer-Generated Views

Nathan E. Green, MD, S.-Y. James Chen, PhD, Adam R. Hansgen, John C. Messenger, MD, Bertron M. Groves, MD, and John D. Carroll,* MD

The goal of this study was to determine the severity of vessel foreshortening in standard angiographic views used during percutaneous coronary intervention (PCI). Coronary angiography is limited by its two-dimensional (2D) representation of three-dimensional (3D) structures. Vessel foreshortening in angiographic images may cause errors in the assessment of lesions or the selection and placement of stents. To date, no technique has existed to quantify these 2D limitations or the performance of physicians in selecting angiographic views. Stent deployment was performed in 156 vessel segments in 149 patients. Using 3D reconstruction models of each patient's coronary tree, vessel foreshortening was measured in the actual working view used for stent deployment. A computer-generated optimal view was then identified for each vessel segment and compared to the working view. Vessel foreshortening ranged from 0 to 50% in the 156 working views used for stent deployment and varied by coronary artery and by vessel segment within each artery. In general, views of the mid circumflex artery were the most foreshortened and views of the right coronary artery were the least foreshortened. Expert-recommended views frequently resulted in more foreshortening than computer-generated optimal views, which had only 0.5% ± 1.2% foreshortening with < 2% overlap for the same 156 segments. Optimal views differed from the operator-selected working views by ≥ 10° in over 90% of vessels and frequently occurred in entirely different imaging quadrants. Vessel foreshortening occurs frequently in standard angiographic projections during stent deployment. If unrecognized by the operator, vessel foreshortening may result in suboptimal clinical results. Modifications to expert-recommended views using 3D reconstruction may improve visualization and the accuracy of stent deployment. These results highlight the limitations of 2D angiography and support the development of real-time 3D techniques to improve visualization during PCI. *Catheter Cardiovasc Interv 2005;64:451–459.* © 2005 Wiley-Liss, Inc

Key words: coronary angiography; three-dimensional imaging; percutaneous transluminal angioplasty; coronary stenosis

INTRODUCTION

As with any diagnostic test, the clinical utility of invasive coronary angiography is dependent on its ability to identify accurately the presence or absence of obstructive coronary artery disease. During the past 3 decades, discrepancies between coronary angiography and intravascular ultrasound [1,2], physiologic measurements [3,4], angioscopy [5,6], and autopsy [7,8] have highlighted important limitations with the angiographic diagnosis and assessment of atherosclerotic lesions. While these limitations have resulted in the development of other noninvasive diagnostic techniques [9,10], invasive coronary angiography has remained the reference standard for the diagnosis of atherosclerotic disease and the primary imaging technique used for guidance during percutaneous coronary intervention (PCI).

Conventional coronary angiography utilizes radiographic contrast to display a two-dimensional (2D) silhouette of a vessel's three-dimensional (3D) structure. While 2D images display certain vessel characteristics, the combination of vessel tortuosity, overlap, suboptimal projections, and individual anatomic variation may

Division of Cardiology, University of Colorado Health Sciences Center, Denver, Colorado

*Correspondence to: Dr. John D. Carroll, Division of Cardiology, Box B-132, Room 2024, University of Colorado Health Sciences Center, 4200 East Ninth Avenue, Denver, CO 80262.
E-mail: john.carroll@uchsc.edu

Received 10 June 2004; Revision accepted 29 November 2004

DOI 10.1002/ccd.20331
Published online in Wiley InterScience (www.interscience.wiley.com).

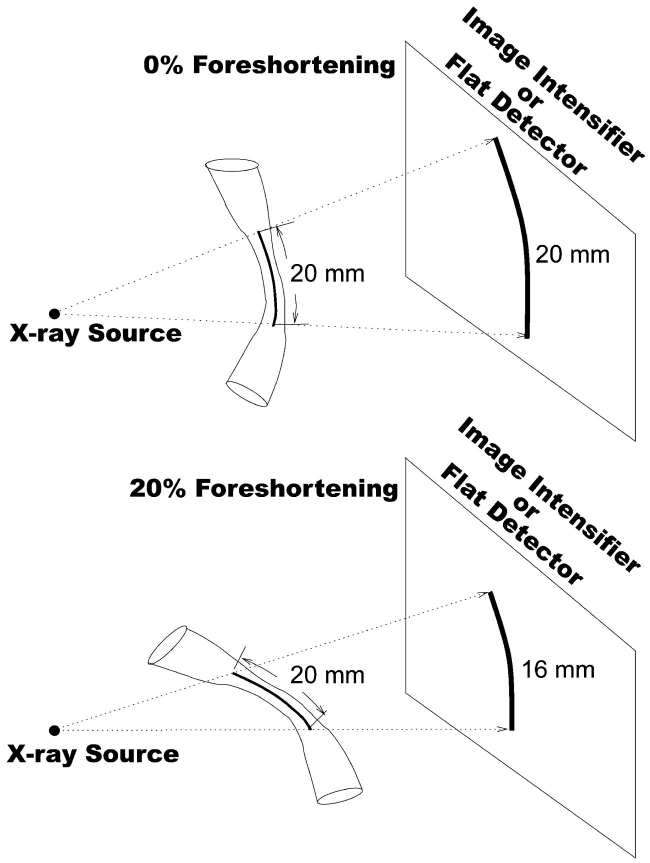

Fig. 1. Simplified model of foreshortening. Perpendicular orientation of the X-ray beam to a vessel segment or lesion of interest results in minimal distortion of the projection image (A). Without perpendicular X-ray beam alignment, vessel foreshortening occurs and results in suboptimal projection images that misrepresent the true length of a lesion or vessel segment (B).

result in insufficient 2D images and may partially account for the suboptimal sensitivity and specificity of coronary angiography [11]. The addition of cranial and caudal angulation to standard oblique views [12,13] resulted in improved visualization and led to the recognition that an optimal view (a projection with the least amount of radiographic vessel foreshortening and radiographic vessel overlap) existed for most vessel segments [14,15]. Expert-recommended or standardized views for coronary angiography [16–22] were subsequently developed to assist in the identification of angiographic views, improve lesion length assessment and quantitative coronary angiography measurements, and assist in
F1 the selection of accurately sized stents (Fig. 1). Because no reliable method has existed to determine the accuracy of standard angiographic views, no objective quantification of vessel foreshortening or overlap during routine coronary angiography and stent deployment exists.

Three-dimensional techniques have been developed to minimize the imaging limitations of 2D angiography [23–26]. In addition to accurately displaying the complexities of coronary anatomy, 3D methods are capable of quantifying vessel curvature, measuring vessel segment length, and identifying the amount of radiographic foreshortening and vessel overlap in any simulated angiographic projection [27–29]. We have previously described and validated an online computer algorithm that produces accurate 3D models from single-, biplane, or rotational angiograms and can be used to identify vessel segment-specific optimal views for coronary intervention [29–34].

In this study, we aimed to determine the amount of foreshortening in the target lesion segment from the angiographic projections chosen for coronary stent deployment by experienced interventional cardiologists. With 3D coronary reconstruction, we measured the amount of vessel segment foreshortening in the working view used for stent deployment. Then we compared the working view to a computer-generated optimal view with both the least amount of image foreshortening and overlap. Differences between these views were then used to define angiographic projections with improved visualization when compared to traditional expert-recommended views.

MATERIALS AND METHODS

Patients

Consecutive patients referred for percutaneous coronary stent implantation from January 2002 to December 2002 were eligible for inclusion in this study. Angiograms were selected for inclusion in this study from patients who underwent coronary stent deployment in the proximal or mid left anterior descending (LAD), the proximal or mid circumflex (CX) artery, obtuse marginal branches, or the proximal, mid, or distal right coronary artery (RCA). Patients with a prior history of coronary artery bypass graft surgery or cardiac transplantation (n = 26), with acutely or chronically occluded vessels (n = 54), or with ostial stenoses, anomalous coronary arteries, or other treated vessels (n = 46) were excluded. In addition, 19 angiograms that were technically insufficient for 3D reconstruction were excluded. The final study cohort for this series consisted of 156 angiograms acquired during stent deployment in 149 patients; 6 patients underwent multivessel PCI. This retrospective analysis was approved by the Colorado Multiple Institutional Review Board.

Coronary Angiography and Stent Deployment

Cineangiograms were obtained with single-plane digital angiographic systems (Integris H3000 System or Integris Allura System, Philips Medical Systems, Andover, MA). Images were acquired at 15 or 30 frames/sec using standard or rotational angiographic techniques [35]. Gantry information, including field of view, gantry angle, and focal spot to image intensifier distance, was recorded with each DICOM image file. After diagnostic angiography was completed, coronary stent deployment was performed by one of four experienced interventional cardiologists according to the operator's customary fashion. Two of the interventional cardiologists each had over 10 years of angiographic imaging experience (combined experience of 40 years) and performed one-half of the procedures. The other two interventional cardiologists each had less than 10 years of experience (combined experience of 14 years). Six different stent types ranging in length from 8 to 30 mm were used. All imaging analyses were performed after completion of the procedure.

Three-Dimensional Reconstruction and Analysis

The 3D reconstruction algorithm has been previously described and validated [27,29,31,32]. Briefly, two angiographic projections with complete opacification of the coronary tree were selected and transferred to a computer workstation (Indigo2; Silicon Graphics, Mountain View, CA) for 3D reconstruction. Then, using the previously described algorithm, a 3D model of each patient's coronary arterial tree was constructed for analysis [32,34]. The angiographic projection selected by the interventional cardiologist and used to document coronary stent deployment (the working view) was identified from the patients' cineangiography. The gantry angles used for the working view were recorded and the treated coronary segment was recorded and classified according to the Bypass Angioplasty Revascularization Investigation (BARI) coronary artery classification scheme [36]. Then, the 3D model was rotated to the gantry angles of the working view. The treated vessel segment was manually identified on the computer workstation using the length (mm) of the stent deployed in each vessel segment. The amount of radiographic vessel foreshortening (%) of the stented segment was determined by the computer algorithm. An optimal view of the same treated segment was generated by the computer algorithm and the gantry angles, foreshortening (%), and vessel overlap (%) in the optimal view were recorded. Previously published studies using phantom models and patient angiograms have confirmed the accuracy of this algorithm to predict angiographic appearances in any projection image [29,34].

Statistical Analysis

All data are expressed as mean ± SD for continuous variables and frequencies or percentages for discrete variables. The differences between groups were assessed by the *t*-test for continuous variables. A P value < 0.05 was considered statistically significant.

TABLE I. Study Population Characteristics

Patients (n = 149)	
Age (years)	59 ± 12
Male (%)	72
Vessels (n = 156)	
LAD proximal (n)	32
LAD mid (n)	35
CX proximal (n)	4
CX mid (n)	18
OM (n)	14
RCA proximal (n)	11
RCA mid (n)	26
RCA distal (n)	16
Stents (n = 176)	
Diameter (mm)	3.42 ± 0.50
Length (mm)	16.10 ± 5.02

RESULTS

The baseline clinical and angiographic characteristics are displayed in Table I. T1

Vessel Foreshortening in Operator-Selected Working Views

Image foreshortening of the 156 vessel segments ranged from 0 to 50% in the working views selected for stent deployment. For a 16 mm vessel segment, 50% image foreshortening would result in an apparent 8 mm vessel segment. Angiographic views used during stent deployment in the circumflex artery had the most foreshortening (mean, 14.1% ± 11.7%; range, 0–50%), while right coronary artery working views had minimal amounts of foreshortening (5.2% ± 6.2%; range, 0–32%; Fig. 2). The severity of foreshortening also varied by the F2
vessel segment treated (Fig. 3). No statistically significant F3
difference in the severity of vessel foreshortening existed between the four individual cardiologists.

In Figure 4, the frequency of 0–10%, 11–19%, or $\geq$ F4
20% foreshortening present in the working view is displayed for each vessel. In all, 26 (17%) of 156 stented segments had $\geq$ 20% foreshortening and an additional 31 segments (20%) had 11–19% foreshortening in the views selected for stent deployment. Working views of the RCA had the least amount of foreshortening while imaging of the CX was the most challenging, with one-third of working views foreshortened by $\geq$ 20%.

The use of general categories of gantry position [left anterior oblique (LAO)-cranial, right anterior oblique (RAO)-caudal, etc.] for specific vessel segments produced significant variation in the degree of foreshortening (Fig. 5). The LAO projection with cranial (CRA) F5
angulation was frequently selected as the working view for proximal and mid LAD interventions and resulted

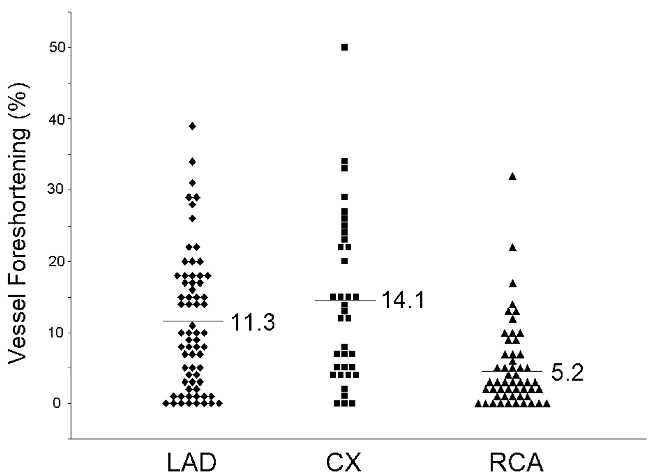

Fig. 2. The mean value and range of vessel foreshortening (%) present in each working view used for stent deployment in the LAD (diamonds), CX (squares), and RCA (circles).

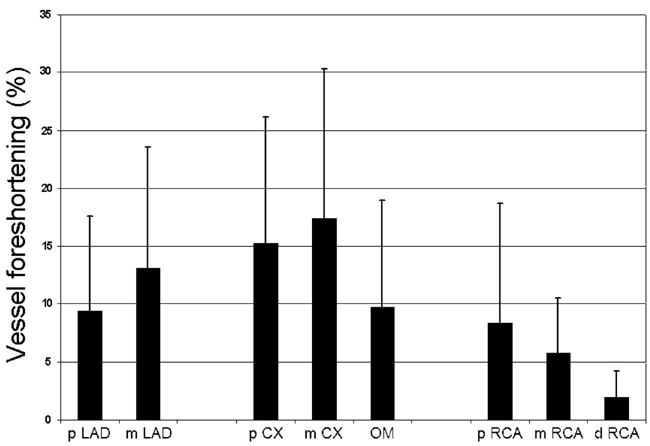

Fig. 3. Vessel foreshortening by BARI segment in the chosen working view (mean ± SD).

in more foreshortening than other projections. For the RCA, the LAO projection with shallow CRA or shallow caudal (CAU) angulation was used almost exclusively for working views and resulted in minimal degrees of foreshortening.

Computer-Generated Views vs. Physician-Determined Views

An optimal view with the least amount of foreshortening and overlap was able to be generated for each vessel segment by the computer algorithm (Fig. 6). In contrast to the working views selected by the interventional cardiologist, the computer-generated views had 0.5% ± 1.2% foreshortening (range, 0–6%) and 1.7% ± 3.2% overlap (range, 0–18%). Of the 156 vessel segments, the computer was able to identify views with ≤ 3% foreshortening in 93%. Furthermore, the optimal view generated by the computer differed from

F6

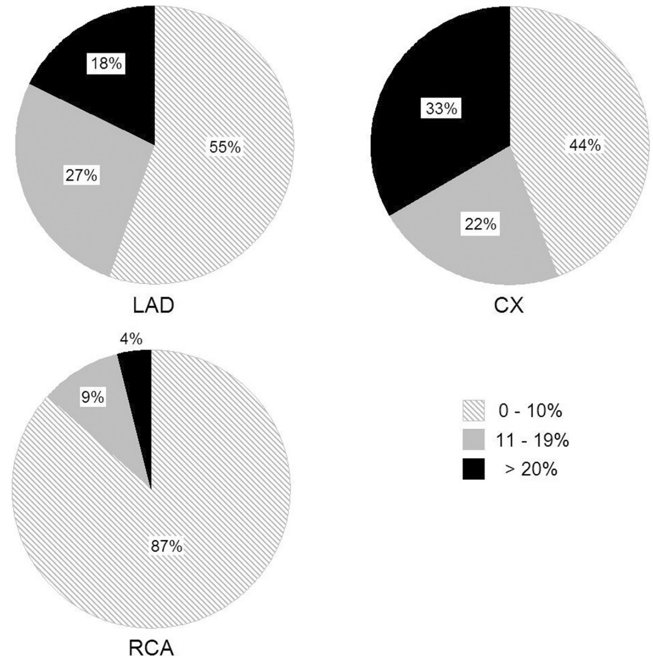

Fig. 4. The proportion of working views with 0–10%, 11–19%, and ≥ 20% vessel foreshortening in the LAD, CX, and RCA.

the working view selected by the interventional cardiologist by $\geq 10^\circ$ in 141 (90.4%) of the 156 procedures. When classified by the quadrant (RAO-CRA, LAO-CAU, etc.) in which the working view was obtained, the computer identified an optimal view in an entirely different quadrant in 73 (47%) of cases.

Figures 7 and 8 compare the working views used for stent deployment and the optimal views generated by the computer algorithm. In general, optimal views had greater degrees of RAO projection for the LAD and more caudal angulation for the RCA when compared with the selected working views. For the circumflex, the optimal views occurred most commonly in the LAO-CAU projection. As the variability of views used for the same vessel segments demonstrates, each view was independently selected and modified by the interventional cardiologist to optimize imaging during stent deployment. When categorized by BARI vessel segment, additional differences between the optimal and working views were evident. For the mid LAD, the working views chosen by the interventional cardiologist tended to have more LAO orientation than the optimal RAO-CAU projection identified by the computer algorithm (Fig. 8). F7 F8

To determine the accuracy of expert-recommended views, a composite of expert-recommended views for specific vessel segments was derived from published guidelines [16–22]. Use of the composite view for each vessel segment in this series resulted in significant image foreshortening, which frequently exceeded

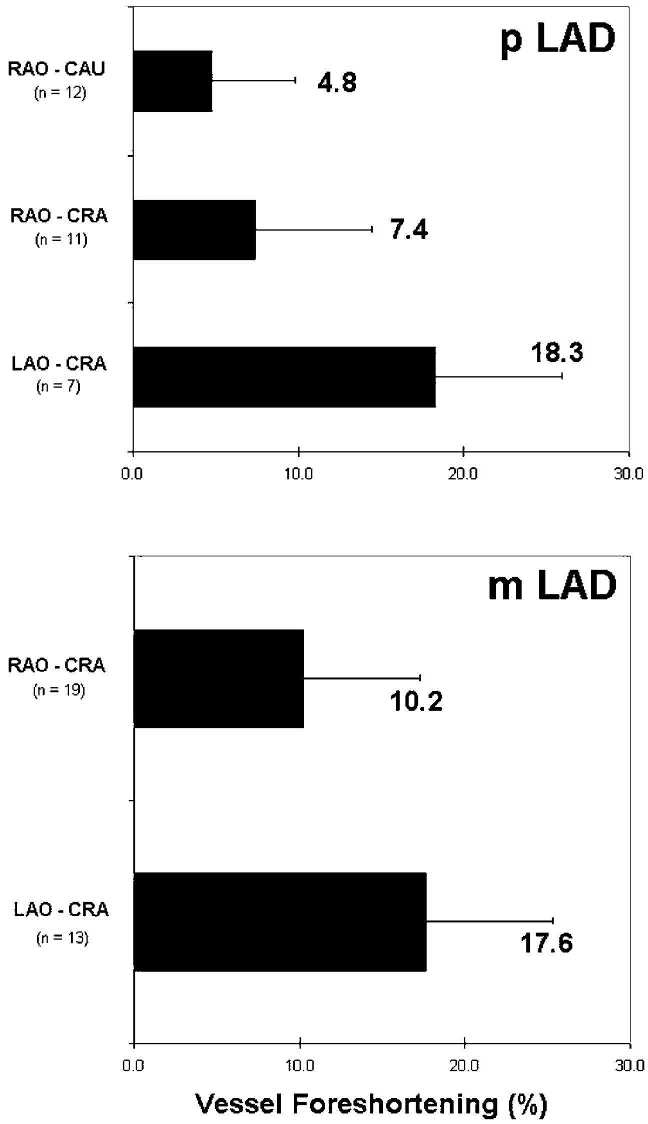

Fig. 5. In the proximal (top) and mid (bottom) LAD, commonly used views resulted in variable degrees of vessel foreshortening (mean). The RAO-CAU view had the least amount of foreshortening for the proximal LAD ($P < 0.001$ vs. LAO-CRA view), while the RAO-CRA view had the least foreshortening in the mid LAD ($P < 0.03$ vs. LAO-CRA view).

T2 20% (Table II). While the LAO-CRA view for the proximal and mid LAD resulted in large amounts of foreshortening, the RAO-CRA view resulted in lesser foreshortening. Similarly, the RAO-CAU view for the mid CX and LAO 60 view for the proximal RCA resulted in large amounts of foreshortening.

DISCUSSION

The ability to evaluate the proficiency of cardiologists in finding the appropriate patient-specific angiographic view for coronary stent placement has previously not existed. In this study, we used a 3D technique to evaluate the performance of individual cardiologists and to determine the accuracy of expert-recommended views that have been accepted and published without objective or quantitative validation. To our knowledge, this is the first study to demonstrate the inaccuracy of subjectively chosen views and the limitations of expert-recommended angiographic views.

In this series, vessel foreshortening ranged from 0 to 50% in the working views selected by experienced interventional cardiologists. While most views of the RCA had minimal amounts of foreshortening, over 40% of views used for stent placement in the mid circumflex were foreshortened by more than 20%. Foreshortening in views of the LAD varied between 0 and 39% and was highly dependent on the chosen gantry angle. Importantly, the computer algorithm was able to identify better views with less than 3% foreshortening in over 90% of vessel segments. These data suggest that the 2D imaging limitations of conventional coronary angiography are unrecognized and more prevalent than previously realized.

Expert-recommended views were initially published to guide invasive cardiologists in the efficient selection of optimal angiographic projections while minimizing contrast and radiation usage. While several reports have subjectively demonstrated improvements in visualization with standard views [14,15], no scientific measurement of the accuracy of expert-recommended views has ever been published. Using an objective 3D method, our data suggest that modifications of expert-recommended views may further improve imaging accuracy during diagnostic and therapeutic angiography with the caveat that anatomical variations necessitate some individualization of views. Specifically, the addition of shallow (10–15°) caudal angulation to the standard LAO projection may result in less foreshortening of RCA working views. For the circumflex and obtuse marginal (OM) branches, the traditional RAO-caudal view results in significant amounts of vessel foreshortening. Our data suggest that replacement of these traditional views with an LAO-caudal projection will result in less foreshortening. Because of its anatomic orientation, optimal imaging of the proximal and mid LAD can be challenging. In our series, working views that appeared to be optimal actually had significant amounts of foreshortening that was imperceptible to the operator and difficult to recognize retrospectively when viewing the angiographic data. While the RAO-caudal projection resulted in the least amount of foreshortening for the proximal LAD, the practical use of this view is also dependent on avoiding overlap from high diagonal branches. For the mid LAD, a 20–30° RAO orientation with 20° cranial

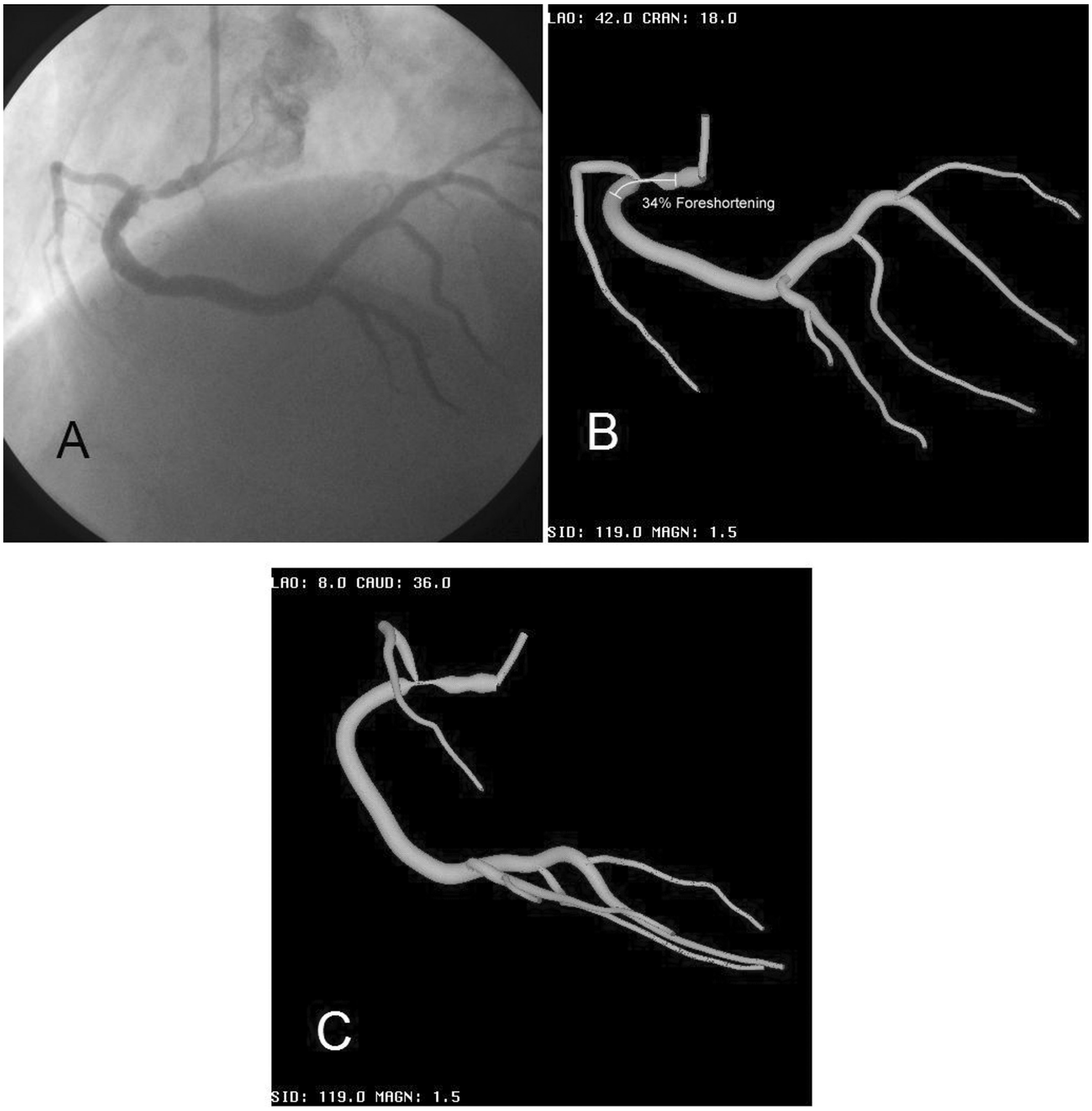

Fig. 6. Determination of the working view vs. the optimal view. The angiographic working view (LAO 42, CRA 18) used for stent deployment in the proximal RCA appears to display the lesion without foreshortening (A). After 3D reconstruction of the vessel, rotation to the working view gantry angles, and selection of the 18 mm stented segment, the computer identified 34% foreshortening in the working view (B). The computer-generated optimal view (LAO 08, CAU 36) demonstrates 0% foreshortening in the proximal RCA (C). Note the misrepresentation of the origin of the conus branch in the working view vs. optimal view. [Color figure can be viewed in the online issue, which is available at www.interscience.wiley.com]

angulation resulted in less foreshortening than views with LAO orientation. In many cases, the variable anatomy of the proximal and mid LAD combined with the variable orientation of the heart in the thorax make the identification of a generalized recommended view for these vessel segments especially challenging.

The amount of unappreciated vessel foreshortening is an important surrogate measure of outcome for studying performance in percutaneous X-ray-based vascular interventions. Inaccurate imaging during therapeutic procedures may result in the selection of a stent that is too short and misses the lesion, or overtreatment with a long stent that increases the risk of restenosis [37,38], creates a hinge point [39], covers a side branch, or results in an edge dissection [40,41]. While this study did not assess whether clinical outcomes from these interventions were compromised because of the chosen angiographic views, further investigations to determine if 3D imaging can impact clinical outcomes are warranted.

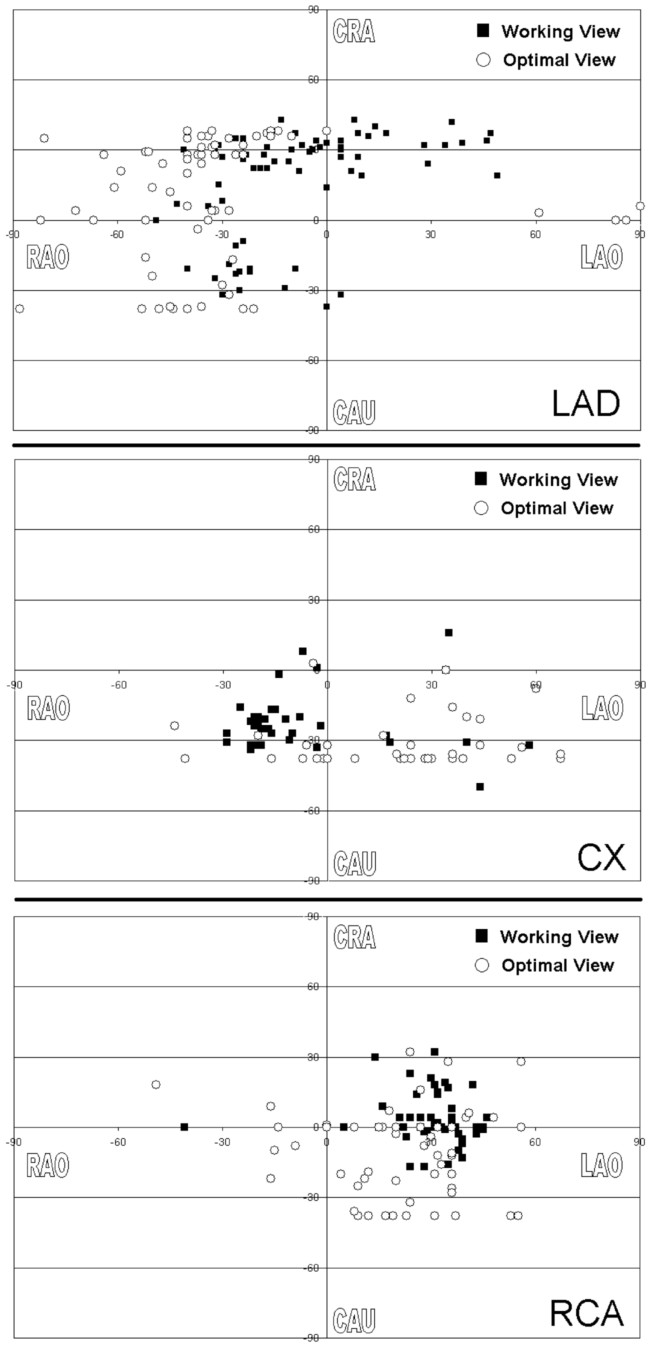

Fig. 7. View maps of the LAD, CX, and RCA divided into quadrants (LAO-CRA, LAO-CAU, RAO-CAU, and RAO-CRA). Differences between the actual working view (filled square) and the computer-generated optimal view (open circle) for each of the 156 vessel segments are apparent.

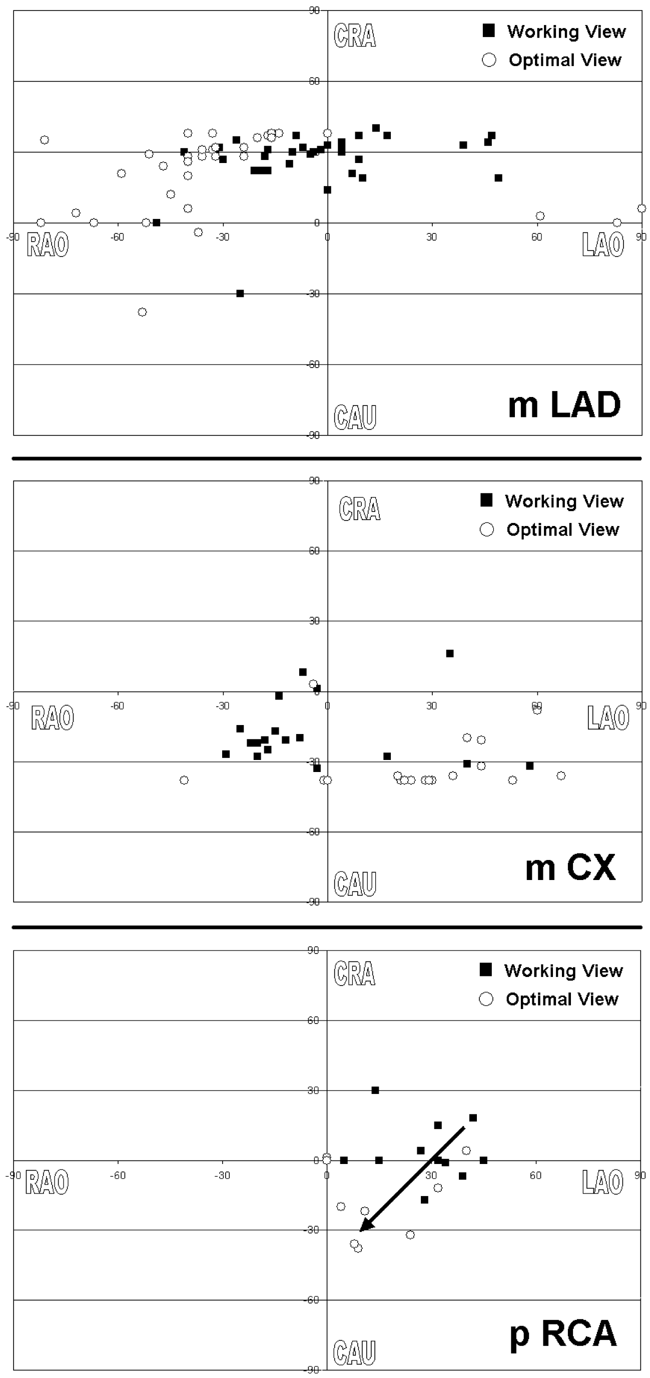

Fig. 8. Differences between the working (filled square) and optimal (open circle) views for the mid LAD (top), mid circumflex (middle), and proximal RCA (bottom). The optimal view frequently occurred in different quadrants from the working view (arrow; matched working and optimal view of the same patient as in Fig. 4).

The selection of a working view incorporates many clinical, technical, and procedural variables and may differ from a computer-generated optimal view. Different working views may be used at different times during a procedure to visualize specifically downstream flow, the distal end of a stent, or other clinically relevant characteristics. A computer-generated view that only solves the foreshortening or overlap problems may be suboptimal because of other variables not included by the algorithm. For example, the imaging

TABLE II. Vessel Foreshortening in Expert-Recommended Views

Vessel	n	Composite view	% foreshortening (± SD)
p LAD	32	LAO 40, CRA 20	44.0 ± 14.9
		RAO 10, CAU 20	20.2 ± 17.9
m LAD	35	RAO 10, CRA 30	10.4 ± 8.9
		LAO 40, CRA 20	39.0 ± 17.0
p CX	4	LAO 50, CAU 20	1.0 ± 2.0
m CX	18	RAO 30, CAU 20	27.6 ± 12.3
OM	14	RAO 30, CAU 20	18.5 ± 13.3
p RCA	11	LAO 60	23.4 ± 16.9
m RCA	26	LAO 45	6.3 ± 5.4

equipment may be physically unable to be positioned at a computer-identified angle due to collision with the patient's body or table. Some computer-identified views may be limited by image quality, by visually distracting translational motion such as an RAO view of the right coronary artery, or by pacemaker or defibrillator units that obscure visualization.

This study demonstrates that a significant amount of unrecognized vessel foreshortening occurs in the working views selected for stent deployment by experienced interventional cardiologists. In addition to the subjective operator-dependent technique of acquiring views, our results reflect the inherent limitations of 2D angiography and the associated imaging inaccuracies that may be imperceptible to the human eye. Three-dimensional reconstruction techniques provide an objective model from which accurate measurements can be made and optimal views predicted. The extension of this powerful imaging tool into the coronary circulation may result in the use of less radiographic contrast, less radiation, and more precise characterization and treatment of obstructive coronary artery disease.

ACKNOWLEDGMENTS

The authors acknowledge the contributions of Dr. J.E.B. Burchenal and Ms. Kathy Kioussopoulos for the completion of this study. Supported in part by grants from the Blount Scholar Endowed Fellowship (to N.E.G.) and the National Institutes of Health (HL60220; to S.-Y.J.C. and J.D.C.).

REFERENCES

1. Nissen S, Gurley J, Grines C, Booth D, McClure R, Berk M, Fischer C, DeMaria A. Intravascular ultrasound assessment of lumen size and wall morphology in normal subjects and patients with coronary artery disease. Circulation 1991;84:1087–1099.
2. Mintz GS, Painter JA, Pichard AD, Kent KM, Satler LF, Popma JJ, Ya Chien C, Bucher TA, Sokolowicz LE, Leon MB. Atherosclerosis in angiographically ''normal'' coronary artery reference segments: an intravascular ultrasound study with clinical correlations. J Am Coll Cardiol 1995;25:1479–1485.
3. White C, Wright C, Doty D, Hiratza L, Eastham C, Harrison D, Marcus M. Does visual interpretation of the coronary arteriogram predict the physiologic importance of a coronary stenosis? N Engl J Med 1984;310:819–824.
4. Pijls NHJ, de Bruyne B, Peels K, van der Voort PH, Bonnier HJRM, Bartunek J, Koolen JJ. Measurement of fractional flow reserve to assess the functional severity of coronary-artery stenoses. N Engl J Med 1996;334:1703–1708.
5. Ramee SR, White CJ, Collins TJ, Mesa JE, Murgo JP. Percutaneous angioscopy during coronary angioplasty using a steerable microangioscope. J Am Coll Cardiol 1991;17:100–105.
6. Teirstein PS, Schatz RA, DeNardo SJ, Jensen EE, Johnson AD. Angioscopic versus angiographic detection of thrombus during coronary interventional procedures. Am J Cardiol 1995;75: 1083–1087.
7. Schwartz JN, Kong Y, Hackel DB, Bartel AG. Comparison of angiographic and postmortem findings in patients with coronary artery disease. Am J Cardiol 1975;36:174–178.
8. Arnett EN, Isner JM, Redwood CR, Kent KM, Baker WP, Ackerstein H, Roberts WC. Coronary artery narrowing in coronary heart disease: comparison of cineangiographic and necropsy findings. Ann Intern Med 1979;91:350–356.
9. Achenbach S, Giesler T, Ropers D, Ulzheimer S, Derlien H, Schulte C, Wenkel E, Moshage W, Bautz W, Daniel WG, et al. Detection of coronary artery stenoses by contrast-enhanced, retrospectively electrocardiographically-gated, multislice spiral computed tomography. Circulation 2001;103:2535–2538.
10. Kim WY, Danias PG, Stuber M, Flamm SD, Plein S, Nagel E, Langerak SE, Weber OM, Pedersen EM, Schmidt M, et al. Coronary magnetic resonance angiography for the detection of coronary stenoses. N Engl J Med 2001;345:1863–1869.
11. Thomas AC, Davies MJ, Dilly S, Dilly N, Franc F. Potential errors in the estimation of coronary arterial stenosis from clinical arteriography with reference to the shape of the coronary arterial lumen. Br Heart J 1986;55:129–139.
12. Lesperance J, Saltiel J, Petitclerc R, Bourassa MG. Angulated views in the sagittal plane for improved accuracy of cinecoronary angiography. Am J Roentgenol Radium Ther Nucl Med 1974;121:565–574.
13. Sos TA, Baltaxe HA. Cranial and caudal angulation for coronary angiography revisited. Circulation 1977;56:119–123.
14. Elliot LP, Green CE, Rogers WJ, Mantle JA, Papapietro S, Hood WP. The importance of angled right anterior oblique views in improving visualization of the coronary arteries: I, caudocranial view. Radiology 1982;142:631–636.
15. Green CE, Elliot LP, Rogers WJ, Mantle JA, Papapietro S, Hood WP. The importance of angled right anterior oblique views in improving visualization of the coronary arteries: II, craniocaudal view. Radiology 1982;142:637–641.
16. Tilkian AG, Daily EK. 1986. Cardiac catheterization and coronary arteriography. In: Tilkian AG, Daily EK, editors. Cardiovascular procedures: diagnostic techniques and therapeutic procedures. St. Louis, MO: Mosby. p 117–159.
17. Pepine CJ, Lambert CR, Hill JA. 1994. Coronary angiography. In: Pepine CJ, Lambert CR, Hill JA, editors. Diagnostic and therapeutic cardiac catheterization. Baltimore, MD: Williams and Wilkins. p 238–274.
18. Deligonal U, Kern MJ, Roth R. 1999. Angiographic data. In: Kern MJ, editor. The cardiac catheterization handbook. St. Louis, MO: Mosby. p 278–390.
19. Gibson CM, Ryan K, Sparano A, Moynihan JL, Rizzo M, Kelley M, Marble SJ, Laham R, Simons M, McClusky TR, et al. Angiographic methods to assess human coronary angiogenesis. Am Heart J 1999;137:169–179.

20. Baim DS, Grossman W. 2000. Coronary angiography. In: Baim DS, Grossman W, editors. Grossman's cardiac catheterization, angiography, and intervention. Philadelphia: Lippincott Williams and Wilkins. p 211–270.
21. Popma JJ, Bittl J. 2001. Coronary angiography and intravascular ultrasonography. In: Braunwald E, Zipes DP, Libby P, editors. Heart disease: a textbook of cardiovascular medicine. Philadelphia: W.B. Saunders. p 387–421.
22. Carroll JD. 2001. Coronary artery imaging. In: Nissen SE, editor. CathSAP II: catheterization and interventional cardiology self-assessment program. Bethesda, MD: American College of Cardiology Foundation.
23. Wahle A, Wellnhofer E, Mugaragu I, Sauer HU, Oswald H, Fleck E. Assessment of diffuse coronary artery disease by quantitative analysis of coronary morphology based upon 3D reconstruction from biplane angiograms. IEEE Trans Med Imag 1995;14:230–241.
24. Nguyen TV, Sklansky J. Reconstructing the 3D medial axes of coronary arteries in single-view cineangiograms. IEEE Trans Med Imag 1994;13:61–73.
25. Metz CE, Fencil LE. Determination of three-dimensional structures in biplane radiography without prior knowledge of the relationship between two views: theory. Med Phys 1989;16:45–51.
26. Wellnhofer E, Wahle A, Mugaragu I, Gross J, Oswald H, Fleck E. Validation of an accurate method for three-dimensional reconstruction and quantitative assessment of volumes, lengths and diameters of coronary vascular branches and segments from biplane angiographic projections. Int J Cardiac Imaging 1999; 15:339–353.
27. Chen SYJ, Carroll JD, Messenger JC. Quantitative analysis of reconstructed 3D coronary arterial tree and intracoronary devices. IEEE Trans Med Imag 2002;21:724–740.
28. Liao R, Chen SYJ, Green NE, Messenger JC, Hansgen AR, Groves BM, Carroll JD. Three-dimensional analysis of in vivo coronary stent: coronary artery interactions. Int J Cardiac Imaging 2004;20:305–313.
29. Messenger JC, Chen SYJ, Carroll JD, Burchenal JEB, Kioussopoulos K, Groves BM. 3D coronary reconstruction from routine single-plane coronary angiograms: clinical validation and quantitative analysis of the right coronary artery in 100 patients. Int J Cardiac Imaging 2000;16:413–427.
30. Hoffman KR, Metz CE, Chen SYJ. Determination of 3D imaging geometry and object configurations from two biplane views: an enhancement of the Metz-Fencil technique. Med Phys 1995;22:1219–1227.
31. Chen SYJ, Hoffman KR, Carroll JD. Three-dimensional reconstruction of coronary arterial tree based on biplane angiograms. In: Loew MH, Hanson KM, editors. Proc SPIE 1996;2710:103–114.
32. Chen SYJ, Metz CE. Improved determination of biplane imaging geometry from two projection images and its application to three-dimensional reconstruction of coronary arterial trees. Med Phys 1997;24:633–654.
33. Chen SYJ, Carroll JD. 1998. 3D coronary angiography: improving visualization strategy for coronary interventions. In: Reiber JH, van der Wall EE, editors. What's new in cardiovascular imaging? Dordrecht: Kluwer Academic Publishers. p 61–78.
34. Chen SYJ, Carroll JD. 3D reconstruction of coronary arterial tree to optimize angiographic visualization. IEEE Trans Med Imag 2000;19:318–336.
35. Maddux JT, Chen SYJ, Groves BM, Messenger JC, Liao R, Strzelczyk J, Wink O, Carroll JD. A randomized study of the safety and clinical utility of rotational angiography versus standard angiography in the diagnosis of coronary artery disease. Catheter Cardiovasc Interv 2004;62:167–174.
36. Alderman EL, Stadius M. The angiographic definitions of the Bypass Angioplasty Revascularization Investigation study (BARI). Coron Art Dis 1992;3:1189–1207.
37. Kobayashi Y, De Gregorio J, Kobayashi N, Akiyama T, Reimers B, Finci L, Di Mario C, Colombo A. Stented segment length as an independent predictor of restenosis. J Am Coll Cardiol 1999;34:651–659.
38. Mauri L, O'Malley AJ, Cutlip DE, Ho KKL, Popma JJ, Chauhan MS, Baim DS, Cohen DJ, Kuntz RE. Effects of stent length and lesion length on coronary restenosis. Am J Cardiol 2004;93:1340–1346.
39. Phillips PS, Alfonso F, Segovia J, Goicolea J, Hernandez R, Banuelos C, Fernandez-Ortiz A, Perez-Vizcayno MJ, Carlos Macaya M. Effects of Palmaz-Schatz stents on angled coronary arteries. Am J Cardiol 1997;79:191–193.
40. Gyongyosi M, Yang P, Khorsand A, Glogar D. Longitudinal straightening effect of stents is an additional predictor for major adverse cardiac events. J Am Coll Cardiol 2000;35:1580–1589.
41. Colombo A, Stankovic G, Moses JW. Selection of coronary stents. J Am Coll Cardiol 2002;40:1021–1033.